



Offline Policy Optimization with Posterior Sampling

Hongqiang Lin¹, Dongxu Zhang², Yiding Sun², Mingzhe Li¹, Ning Yang³, Haijun Zhang⁴

¹Zhejiang University, ²Xi'an Jiaotong University, ³Institute of Automation, Chinese Academy of Sciences, ⁴University of Science and Technology Beijing

A fundamental challenge in model-based offline reinforcement learning (RL) lies in the trade-off between generalization and robustness against exploitation errors in out-of-distribution (OOD) regions. While OOD samples may capture valid underlying physical dynamics, they also introduce the risk of model exploitation. Existing methods typically address this risk through excessive pessimistic regularization, which ensures robustness but often sacrifices generalization. To overcome this limitation, we propose Posterior Sampling-based Policy Optimization (PSPO), which formulates dynamics modeling as a Bayesian inference process to derive a posterior that explicitly quantifies model fidelity. Through the integration of posterior sampling and constrained policy optimization, our method leverages dynamics-consistent OOD transitions for generalization while ensuring robustness against model exploitation. Theoretically, we formulate Q-value estimation under posterior sampling as a stochastic approximation problem and establish its convergence. We decompose policy optimization into a sequence of constrained subproblems, demonstrating that solving these subproblems guarantees monotonic improvement until convergence. Experiments on standard benchmarks validate that PSPO achieves superior performance compared to state-of-the-art baselines.

Date: May 11, 2026

Correspondence: Ning Yang, ning.yang@ia.ac.cn

1 Introduction

Offline reinforcement learning (RL) [15, 26] learns optimal policies from fixed datasets, avoiding the safety risks associated with online trial-and-error. The primary challenge in offline RL is distribution shift [46, 41], where the learned policy deviates from the support of the behavior policy during policy iteration. This deviation exposes the policy to out-of-distribution (OOD) regions. Unconstrained policy iteration in these OOD regions tends to exploit approximation errors, causing erroneous action selection and performance collapse [20]. Consequently, offline RL involves an inherent trade-off between behavioral regularization and value maximization [30].

In model-based offline RL, this trade-off manifests through the utilization of synthetic transitions. On the one hand, synthesizing dynamics-consistent OOD transitions promotes value maximization by facilitating generalization beyond the offline dataset support. On the other hand, it simultaneously introduces risks of model exploitation [12, 22, 17]. Existing approaches typically mitigate this risk through pessimism, penalizing OOD value estimates based on epistemic uncertainty (e.g., the standard deviation of model predictions) to restrict the policy within the dataset support [43, 37, 31]. However, these pessimistic methods disproportionately favor behavioral regularization to ensure safety, inevitably sacrificing generalization.

Thus, there exists a natural question to be addressed: *Can we design a model-based offline RL algorithm that balances generalization and robustness against model exploitation in OOD regions?*

In this paper, we answer this question in the affirmative by proposing Posterior Sampling-based Policy Optimization (PSPO). Grounded in the Bayesian RL framework [8, 4], PSPO treats dynamics model as a random variable rather than a single point estimate. This probabilistic formulation captures epistemic uncertainty through a posterior distribution over candidate models, allowing the policy to adaptively balance generalization and robustness against model exploitation. Our main contributions are summarized as follows:

Algorithm. PSPO formulates dynamics modeling as a Bayesian inference process. Unlike prior works that rely on fixed posterior assumptions, we derive the posterior $P(T|E)$ conditioned on observed transition evidence E , which explicitly quantifies the learned model’s fidelity to the true dynamics. By performing model rollouts via posterior sampling, PSPO allows the policy to explore dynamics-consistent OOD regions. By evaluating the value of these OOD transitions, PSPO facilitates generalization beyond the offline dataset support. Building on this, we develop a constrained policy optimization algorithm that guarantees stable updates and ensures robustness against OOD exploitation. Notably, PSPO establishes a pessimism-free paradigm, distinguishing itself from prior model-based offline RL approaches (Figure 1).

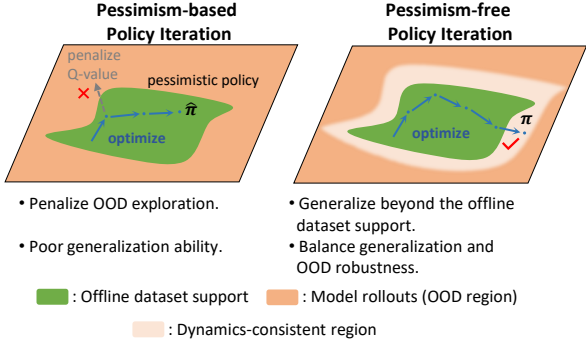


Figure 1: (Left) Existing pessimism-based policy iteration often results in overly pessimistic policies. (Right) We propose a pessimism-free paradigm designed to strike a balance between generalization to dynamics-consistent regions and robustness against model exploitation in OOD regions.

Theoretical Analysis. For posterior sampling process, we present a posterior sampling-based Bellman operator and formulate Q-value estimation as a stochastic approximation problem. We establish that the variance of posterior sampling is bounded and prove the convergence of the estimation process through the Robbins-Monro theorem. For policy optimization, we define a posterior sampling-based Bellman optimality operator and decompose the optimization task into a sequence of constrained subproblems. We prove that solving these subproblems guarantees monotonic improvement with respect to the original objective function until convergence.

Experimental Results. Extensive evaluations across deterministic and stochastic benchmarks demonstrate that PSPO achieves state-of-the-art (SoTA) performance, consistent with our theoretical analysis. Finally, ablation studies verify the efficacy and indispensability of each key component within the PSPO algorithm.

2 Preliminaries and Notations

Bayes-Adaptive Markov Decision Process (BAMDP) BAMDP is the classic framework for sequential decision-making under epistemic uncertainty [9]. A BAMDP is defined by the tuple $\mathcal{M} = (\mathcal{S}, \mathcal{A}, P, r, \rho_0, \gamma)$. Here, \mathcal{S} and \mathcal{A} denote the state and action spaces, respectively, $r : \mathcal{S} \times \mathcal{A} \rightarrow [-R_{\max}, R_{\max}]$ is the bounded reward function, ρ_0 is the initial state distribution, and γ is the discount factor. Crucially, P represents a probabilistic belief over the unknown transition dynamics $T : \mathcal{S} \times \mathcal{A} \rightarrow \Delta(\mathcal{S})$, where $\Delta(\cdot)$ denotes the probability simplex.

Bayesian RL Standard RL aims to find an optimal policy $\pi : \mathcal{S} \rightarrow \Delta(\mathcal{A})$ that maximizes the expected cumulative discounted return: $J(\pi, T) = \mathbb{E}_{\rho_0, \pi, T} [\sum_{t=0}^{\infty} \gamma^t r(s_t, a_t)]$, where T denotes the transition dynamics model. While standard offline approaches typically employ Maximum Likelihood Estimation (MLE) to fit a deterministic point estimate of the dynamics model, modern Bayesian RL treats T as a random variable. Historically, Bayesian inference involves maintaining distributions over model weights. However, in high-dimensional environments, transition dynamics are typically modeled using deep neural networks, and the posterior over network weights resides on a complex manifold, rendering exact inference intractable. To bridge the gap between Bayesian theory and deep RL scalability, modern approaches [5, 33, 10, 34, 6] approximate the posterior over the dynamics model T , rather than over the network weights. Through Bayesian inference, we update the prior $P(T)$ with observed evidence E to obtain the posterior $P(T|E) = \frac{P(T)P(E|T)}{P(E)} \propto P(T)P(E|T)$. Subsequently, Bayesian prediction computes the next-state probability by marginalizing over the model posterior: $P(s'|s, a) = \int_T T(s'|s, a)P(T|s, a)dT$.

3 Formulation

This section presents the formulation of the objective function, the construction of the posterior distribution $P(T|E)$, and the theoretical properties of the sampling process.

3.1 Objective Function

The optimization objective for PSPO is to maximize the expected return averaged over the posterior distribution of the model dynamics:

$$\mathcal{J}(\pi) = \mathbb{E}_{T_0 \sim P(T|\mathcal{D})}^{\rho_0, \pi} \left[\mathbb{E}_{T_1 \sim P(T|\mathcal{D})} \left[\cdots \mathbb{E}_{T_\infty, \pi} \left[\sum_{t=0}^{\infty} \gamma^t r(s_t, a_t) \right] \right] \right]. \quad (1)$$

This formulation explicitly integrates epistemic uncertainty into value estimation by treating the transition dynamics as random variables drawn from the posterior $P(T|E)$.

Under the condition that a model is sampled from the posterior $P(T|E)$ at the beginning of each episode and held fixed for its duration, or if the posterior distribution is a point mass, then Eq. 1 reduces to:

$$\mathcal{J}(\pi) = \mathbb{E}_{\pi, T \sim P(T|E)} [J(\pi, T)]. \quad (2)$$

The policy obtained by maximizing Eq. 2 with respect to π is known as the Bayes-optimal policy [9]. In this paper, we focus on the generalized objective of Bayesian RL defined by Eq. 1, with the proposed algorithm retaining full applicability to the objective in Eq. 2.

3.2 Posterior Distribution $P(T|E)$

The posterior distribution inherently defines the principle by which we utilize the learned models [10]. In the offline setting, the design of this posterior distribution must account for two primary principles:

1. **Adaptability.** The posterior must be adaptable, such that the probability of selecting each dynamics model can be updated through a likelihood function upon observing transition evidence $E = (s, a, r, s')$.
2. **Generalization.** The posterior should encourage exploration by maintaining non-negligible probability mass near the support of the offline dataset.

To satisfy Principle 1, we define an empirical consistency metric as a function of the transition dynamics model T :

$$\mathcal{F}(T) = |Q(s, a) - (r + \gamma \mathbb{E}_{s' \sim T} [V(s')])|^2. \quad (3)$$

Upon observing a new transition (s, a, r, s') , we compute the metric $\mathcal{F}(T_i)$ for each learned dynamics model T_i . We hypothesize that models with smaller $\mathcal{F}(T_i)$ should be assigned greater weight. To identify the optimal weighting among infinite candidates, we invoke the Principle of Minimum Information, which selects the posterior belief that is closest to the prior in terms of information distance while satisfying the constraints imposed by the new evidence. This leads to the following optimization problem:

$$\min_{P(T|E)} D_{\text{KL}}(P(T|E) || P(T)) + \beta \mathbb{E}_{T \sim P(T|E)} [\mathcal{F}(T)], \quad (4)$$

where $\beta > 0$ is hyperparameter. Solving Eq. 4 leads to the posterior distribution: $P(T|E) \propto P(T) \cdot \exp(-\beta \cdot \mathcal{F}(T))$. This solution interprets $P(E|T) \propto \exp(-\beta \cdot \mathcal{F}(T))$ as a generalized likelihood, aligning with the variational framework of generalized Bayesian inference [2]. It is noteworthy that our belief update framework theoretically guarantees exploration (i.e., Principle 2) through Eq. 4. The expectation term $\mathbb{E}_{T \sim P(T|E)} [\mathcal{F}(T)]$

anchors the posterior to models consistent with the offline dataset support. Conversely, the regularization term $D_{\text{KL}}(P(T|E)||P(T))$ enforces exploration by acting as an entropy regularizer that prevents the posterior from collapsing onto a single model. Consequently, the framework automatically satisfies our exploration principle without requiring manual intervention.

3.3 Theoretical Property of Sampling Process

In the Bayesian setting, we define the posterior sampling-based Bellman operator $\bar{\mathcal{B}}^\pi$ to evaluate objective function $\mathcal{J}(\pi)$ (Eq. 1):

$$(\bar{\mathcal{B}}^\pi Q)(s, a) = r(s, a) + \gamma \mathbb{E}_{T \sim P(T|E), s' \sim T, a' \sim \pi} [Q(s', a')]. \quad (5)$$

Proposition 1. *The posterior sampling-based Bellman operator $\bar{\mathcal{B}}^\pi$ is a γ -contraction with respect to the L_∞ -norm.*

Although $\bar{\mathcal{B}}^\pi$ is theoretically a γ -contraction mapping, directly performing value estimation with this operator is computationally intractable due to the expectation over the continuous (or large finite) space of dynamics models. To address this, our algorithm employs a stochastic approximation approach, estimating the update target by sampling models from the posterior $P(T|E)$. While the contraction property ensures the existence of a unique fixed point, the stochastic nature of the updates introduces sampling noise. Consequently, convergence relies on the Robbins-Monro theorem [35], which requires not only a contracting expectation but also a bounded variance of the stochastic estimate. The following theorem establishes this crucial property, proving that the variance of our sampled target is bounded. The complete proof is detailed in Appendix D.

Proposition 2. *Assuming the reward is bounded such that $|r| \leq R_{\max}$, and let $Y_t(s, a)$ be the stochastic target computed at update t : $Y_t = r(s, a) + \gamma \mathbb{E}_{s' \sim T'(\cdot|s, a)} [V_t(s')]$ where $T' \sim P(T|E)$ and $V_t(s') = \mathbb{E}_{a' \sim \pi_t} [Q_t(s', a')]$. Then, the variance of Y_t satisfies $\text{Var}(Y_t) \leq \frac{R_{\max}^2}{(1-\gamma)^2}$.*

Remark 1 (Convergence of Q-value Estimation). *The estimation of Q-values utilizes a stochastic approximation process, with the update rule defined as follows:*

$$Q_{t+1}(s, a) = Q_t(s, a) + \eta_t (Y_t(s, a) - Q_t(s, a)). \quad (6)$$

Given the bounded variance of $Y_t(s, a)$ (Theorem 2) and the γ -contraction property of the operator $\bar{\mathcal{B}}^\pi$ (Proposition 1), the Robbins-Monro theorem guarantees that the evaluation iterates converge to Q^ under the standard learning rate schedule (i.e., $\sum \eta_t = \infty$ and $\sum \eta_t^2 < \infty$).*

Our approach estimates $\mathcal{J}(\pi)$ by sampling dynamics models from the posterior derived in Eq. 4, a pessimism-free mechanism that ensures convergence to Q^* . Beyond convergence, posterior sampling is critical for generalization. We now clarify this sampling process by discussing its theoretical connections to established exploration techniques.

Remark 2 (Connection to Thompson Sampling). *PSPO implements a variant of Thompson Sampling by drawing dynamics models from the posterior $P(T|E)$ to synthesize transitions. Unlike standard ensemble methods that often average predictions, our approach preserves the stochasticity inherent in the posterior variance to translate epistemic uncertainty into controlled exploration. Furthermore, by modulating the posterior using empirical consistency ($\mathcal{F}(T)$, Eq. 3), the algorithm adaptively concentrates probability mass on high-fidelity models. This enables PSPO to selectively leverage dynamics-consistent OOD transitions for effective generalization beyond the offline dataset support, while suppressing hallucinations arising from poorly fitted models.*

4 Posterior Sampling-based Policy Optimization (PSPO)

In this section, we address the optimization of $\mathcal{J}(\pi)$ (Eq. 1) through policy iteration. We then present the complete PSPO algorithm and its implementation.

Algorithm 1 Posterior Sampling-based Policy Optimization

Require: Offline dataset \mathcal{D} , model ensemble size N , iteration steps I .

- 1: **Initialization:** Randomly initialize Q-function $Q_\theta(s, a)$ and policy $\pi_\phi(a|s)$. Initialize the target Q-function $Q_{\theta'}(s, a)$ by setting its parameters θ' to the current Q-network parameters θ , and initialize the target policy $\pi_{\phi'}(a|s)$ by setting $\phi' \leftarrow \phi$. Randomly initialize N dynamics models $\{T_{\psi_i}(s'|s, a)\}_{i=1}^N$.
- 2: **Dynamics model training:** Train each dynamics model $T_{\psi_i}(s'|s, a)$ to maximize:

$$\mathbb{E}_{(s_t, a_t, r_{t+1}, s_{t+1}) \sim \mathcal{D}} [\log T_{\psi_i}(s_{t+1}, r_{t+1} | s_t, a_t)].$$

- 3: **for** $i = 1, 2, \dots, I$ **do**
 - 4: **Constructing posterior belief** $P(T|E)$: The posterior belief $P(T|E)$ over the dynamics model is obtained by solving Eq. 4.
 - 5: **Policy evaluation:** Execute the evaluation step according to Eq. 8 to update Q_θ .
 - 6: **Policy improvement:** Execute the improvement step according to Eq. 9 to update policy $\pi_\phi(a|s)$.
 - 7: **Moving average:** Update target Q-function $Q_{\theta'}$ and reference policy $\pi_{\phi'}$.
 - 8: **end for**
 - 9: **return** π_ϕ .
-

4.1 Iterative Regularized Policy Optimization

Optimizing the objective function $\mathcal{J}(\pi)$ (Eq. 1) without resorting to pessimism (e.g., uncertainty penalization of the Q-function) requires addressing two key challenges:

1. Regulate OOD exploration to maintain adherence to the offline dataset support, effectively mitigating distribution shift while permitting safe exploration.
2. Alleviate optimization instability stemming from the non-stationary state visitation distribution induced by time-varying dynamics and evolving policies.

To mitigate the first challenge, we augment the objective function with a regularization term that prevents the policy from excessively sampling OOD actions. Letting μ denote the reference policy and $\alpha > 0$ denote the regularization strength, we consider the following regularized objective:

$$\tilde{\mathcal{J}}(\pi) = \mathbb{E}_{T_0 \sim P(T|\mathcal{D})}^{\rho_0, \pi} \left[\mathbb{E}_{T_1 \sim P(T|\mathcal{D})}^{\rho_0, \pi} \left[\dots \mathbb{E}_{T_\infty, \pi}^{\rho_0, \pi} \left[\sum_{t=0}^{\infty} \gamma^t (r(s_t, a_t) - \alpha D_{\text{KL}}(\pi(\cdot|s_t) || \mu(\cdot|s_t))) \right] \right] \right], \quad (7)$$

where $D_{\text{KL}}(\pi || \mu)$ serves as a soft constraint, explicitly modulating the trade-off between reward maximization and behavior regularization.

To evaluate $\tilde{\mathcal{J}}(\pi)$, we propose the following posterior sampling-based Bellman optimality operator:

$$(\tilde{\mathcal{B}}^* Q)(s, a) = r(s, a) + \gamma \mathbb{E}_{T \sim P(T|E), s' \sim T} \left[\alpha \log \mathbb{E}_\mu \exp \left(\frac{Q(s', a')}{\alpha} \right) \right]. \quad (8)$$

Formally, we have the following theorem:

Theorem 1. *Starting from any function $Q : \mathcal{S} \times \mathcal{A} \rightarrow \mathbb{R}$ and iteratively applying posterior sampling-based Bellman optimality operator $\tilde{\mathcal{B}}^*$, the resulting sequence converges to \tilde{Q}^* . The optimal policy for the objective $\tilde{\mathcal{J}}(\pi)$ is then obtained from this fixed point as: $\pi^*(a|s) \propto \mu(a|s) \exp \left(\frac{1}{\alpha} \tilde{Q}^*(s, a) \right)$.*

To address the second challenge, we limit the magnitude of policy updates. Let π_i denote the policy obtained at the i -th iteration. We consider the following optimization problem:

$$\pi_{i+1} = \arg \max_{\pi} \tilde{\mathcal{J}}(\pi), \quad \text{s.t.} \quad D_{\text{KL}}(\pi || \pi_i) \leq \epsilon. \quad (9)$$

Since Eq. 9 optimizes the regularized objective function $\tilde{\mathcal{J}}(\pi)$, a natural question arises: Does solving Eq. 9 guarantee improvement of the original objective function $\mathcal{J}(\pi)$? The following theorem addresses this question.

Theorem 2. *Let $C_{\text{KL}}(\pi) = \mathcal{J}(\pi) - \tilde{\mathcal{J}}(\pi)$ denote the regularization term, and let $F = F(\pi_i)$ be the Fisher Information Matrix at π_i . If ϵ is sufficiently small and the condition $\|\nabla \mathcal{J}(\pi_i)\|_F^2 > \langle \nabla \mathcal{J}(\pi_i), \nabla C_{\text{KL}}(\pi_i) \rangle_F$ holds, then starting from an arbitrary policy π_0 , the sequence of policies $\{\pi_i\}_{i \geq 0}$ generated by iteratively solving Eq. 9 guarantees monotonic improvement of $\mathcal{J}(\pi)$, such that $\mathcal{J}(\pi_{i+1}) \geq \mathcal{J}(\pi_i)$.*

Remark 3 (Monotonic Improvement). *Theorem 2 establishes that the policy sequence $\{\pi_i\}_{i \geq 0}$ improves monotonically with respect to the objective $\mathcal{J}(\pi_i)$ defined in Eq. 1. Together with Theorem 1, the sequence converges to the optimal policy: $\pi^*(a|s) \propto \mu(a|s) \exp(\frac{1}{\alpha} \bar{Q}^*(s, a))$.*

Remark 4 (Connection to the Expectation-Maximization (EM) algorithm). (1). *E-Step: The posterior $P(T|E)$ evaluates the quality of each dynamics model, assigning them proportional selection probabilities. Because its metric $\mathcal{F}(T)$ depends on the current critic (Q, V) , these probabilities must dynamically update to reflect model consistency under the evolving policy.* (2). *M-Step: Holding the current $P(T|E)$ fixed, we update the policy. Theorems 1 and 2 provide the theoretical justification that this update step yields monotonic improvement.*

Crucially, the divergence constraint between π and μ is introduced exclusively to ensure optimization stability, rather than to induce pessimism. Our experiments further validate this design: while PSPO’s value estimates do not strictly constitute a lower bound on true returns (thus avoiding explicit pessimism), the absence of this stability constraint significantly degrades performance.

4.2 Algorithm and Implementation

Building upon the theoretical analysis established in the preceding subsection, we present the practical implementation of Posterior Sampling-based Policy Optimization (PSPO). PSPO optimizes the policy by leveraging dynamics models sampled from the posterior distribution $P(T|E)$. The procedure is detailed in Algorithm 1.

Dynamics Model Learning While the transition dynamics are theoretically treated as a random variable following a continuous distribution, maintaining such a distribution is computationally intractable. To bridge this gap, we approximate the posterior using a model ensemble, where each member is trained via MLE (details in Appendix A and Appendix E.3). Under a uniform prior, Eq. 3 and Eq. 4 are applied sequentially to each ensemble member, yielding a computationally efficient yet principled posterior approximation.

Policy Iteration We parameterize the Q-function and the policy using neural networks Q_θ and π_ϕ , where θ and ϕ denote their respective parameters. To enhance training stability, we employ target networks with soft updates [25]. Following standard practice, we set the reference policy μ to the behavior policy used to collect the dataset. We augment the offline dataset \mathcal{D} with the model-generated dataset $\hat{\mathcal{D}}$ to effectively generalize the policy beyond the offline dataset support [22]. Policy evaluation is then performed based on the posterior sampling-based Bellman optimality operator (Eq. 8). For policy improvement, we reformulate the constrained optimization in Eq. 9 into an unconstrained problem via the Karush-Kuhn-Tucker (KKT) conditions.

5 Experiments

Our experimental evaluation focuses on addressing the following four primary research questions:

Q1: Performance Evaluation. What is the empirical performance of PSPO compared to SoTA offline RL algorithms?

Q2: Theoretical Consistency. Do the empirical results align with our theoretical findings, particularly when deep neural networks are employed as function approximators?

Q3: Ablation Study. How does each component of PSPO contribute to overall performance?

Table 1: Performance comparison on D4RL datasets. Scores are normalized as $(\text{score} - \text{random}) / (\text{expert} - \text{random})$ and presented as mean \pm standard deviation. Our results are averaged across 4 random seeds.

Dataset	CQL	DMG	EPQ	MOREL	RAMBO	PMDB	ADM	PSPO (Ours)
HalfCheetah-Random	31.3 \pm 3.5	28.8 \pm 1.3	33.0 \pm 2.4	38.9 \pm 1.8	39.5 \pm 3.5	37.8 \pm 0.2	45.4\pm2.8	37.7 \pm 0.5
HalfCheetah-Medium	46.9 \pm 0.4	54.9 \pm 0.2	67.3 \pm 0.5	60.7 \pm 4.4	77.9 \pm 4.0	75.6 \pm 1.3	72.2 \pm 0.6	79.3\pm0.9
HalfCheetah-Expert	97.3 \pm 1.1	95.9 \pm 0.3	107.2\pm0.2	8.4 \pm 11.8	79.3 \pm 15.1	105.7 \pm 1.0	89.4 \pm 26.4	93.3 \pm 0.6
HalfCheetah-Medium-Expert	95.0 \pm 1.4	91.1 \pm 4.2	95.7 \pm 0.3	80.4 \pm 11.7	95.4 \pm 5.4	108.5 \pm 0.5	103.7 \pm 0.2	109.7\pm1.6
HalfCheetah-Medium-Replay	45.3 \pm 0.3	51.4 \pm 0.3	62.0 \pm 1.6	44.5 \pm 5.6	68.7 \pm 5.3	71.7 \pm 1.1	67.6 \pm 3.4	78.4\pm0.8
HalfCheetah-Full-Replay	76.9 \pm 0.9	79.9 \pm 1.2	85.3 \pm 0.7	70.1 \pm 5.1	87.0 \pm 3.2	90.0 \pm 0.8	86.3 \pm 1.7	94.9\pm1.2
Hopper-Random	5.3 \pm 0.6	20.4 \pm 10.4	32.1 \pm 0.3	38.1\pm10.1	25.4 \pm 7.5	32.7 \pm 0.1	32.7 \pm 0.2	31.9 \pm 0.6
Hopper-Medium	61.9 \pm 6.4	100.6 \pm 1.9	101.3 \pm 0.2	84.0 \pm 17.0	87.0 \pm 15.4	106.8 \pm 0.2	107.4 \pm 0.6	108.5\pm1.3
Hopper-Expert	106.5 \pm 9.1	111.5 \pm 2.2	112.4 \pm 0.5	80.4 \pm 34.9	50.0 \pm 8.1	111.7 \pm 0.3	102.3 \pm 11.9	116.6\pm1.2
Hopper-Medium-Expert	96.9 \pm 15.1	110.4 \pm 3.4	108.8 \pm 5.2	105.6 \pm 8.2	88.2 \pm 20.5	111.8 \pm 0.6	112.7 \pm 0.3	112.8\pm1.4
Hopper-Medium-Replay	86.3 \pm 7.3	101.9 \pm 1.4	97.8 \pm 1.0	81.8 \pm 17.0	99.5 \pm 4.8	106.2 \pm 0.6	104.4 \pm 0.4	110.0\pm1.1
Hopper-Full-Replay	101.9 \pm 0.6	106.4 \pm 1.1	108.5 \pm 0.6	94.4 \pm 20.5	105.2 \pm 2.1	109.1 \pm 0.2	108.5 \pm 0.7	112.5\pm1.6
Walker2d-Random	5.4 \pm 1.7	4.8 \pm 2.2	23.0\pm0.7	16.0 \pm 7.7	0.0 \pm 0.3	21.8 \pm 0.1	22.2 \pm 0.2	22.1 \pm 0.1
Walker2d-Medium	79.5 \pm 3.2	92.4 \pm 2.7	87.8 \pm 2.1	72.8 \pm 11.9	84.9 \pm 2.6	94.2 \pm 1.1	93.2 \pm 1.1	103.9\pm2.5
Walker2d-Expert	109.3 \pm 0.1	114.7 \pm 0.4	109.8\pm1.0	62.6 \pm 29.9	1.6 \pm 2.3	115.9 \pm 1.9	5.5 \pm 1.3	109.8\pm1.4
Walker2d-Medium-Expert	109.1 \pm 0.2	114.4 \pm 0.7	112.0 \pm 0.6	107.5 \pm 5.6	56.7 \pm 39.0	111.9 \pm 0.2	114.9 \pm 0.3	116.1\pm1.0
Walker2d-Medium-Replay	76.8 \pm 10.0	89.7 \pm 5.0	85.3 \pm 1.0	40.8 \pm 20.4	89.2 \pm 6.7	79.9 \pm 0.2	95.6 \pm 2.1	97.0\pm1.4
Walker2d-Full-Replay	94.2 \pm 1.9	97.5 \pm 4.6	107.4 \pm 0.6	84.8 \pm 13.1	88.3 \pm 4.9	95.4 \pm 0.7	99.9 \pm 3.6	107.8\pm1.2
Average	73.7	81.5	85.4	65.1	68.0	88.2	81.3	91.2

Table 2: Performance comparison on offline optimal liquidation task.

Methods	PSPO (Ours)	PMDB	1R2R	ORAAC	RAMBO	CQL	IQL	MOPO	COMBO
Score	102.3\pm1.5	85.5 \pm 2.3	78.8 \pm 1.6	0.0 \pm 0.0	99.6 \pm 0.6	89.4 \pm 1.3	0.0 \pm 0.0	64.7 \pm 21.8	55.0 \pm 29.0

To comprehensively address these questions, we conduct extensive evaluations on the D4RL benchmark [7] and the challenging offline optimal liquidation environment [1, 34]. Detailed hyperparameter settings and environmental configurations are specified in Appendix E.

5.1 Performance Evaluation (Q1)

To answer Q1, we benchmark PSPO against leading model-free (e.g., CQL [14], EPQ [19], DMG [23]) and model-based approaches (e.g., MOREL [12], RAMBO [33], PMDB [10], ADM [17]). As shown in Table 1, PSPO achieves superior performance on 14 datasets and remains competitive on the remaining 4. Results are sourced from original papers or reproduced using official configurations where necessary. Notably, PSPO demonstrates substantial gains on datasets containing a limited number of high-quality trajectories (e.g., “medium”, “medium-expert”, and “full-replay”). To further assess the results, a paired t-test against the strongest baseline (PMDB) yields $t = 2.019$ and $p \approx 0.029$, confirming that the observed improvements are statistically significant at the 5% level.

5.2 Theoretical Consistency (Q2)

Pessimism-free Figure 2 demonstrates that PSPO effectively avoids excessive pessimism, as evidenced by model-predicted returns consistently exceeding actual performance while maintaining monotonic improvement. These results empirically validate Theorems 1 and 2, confirming that our divergence constraint serves to stabilize optimization and prevent model exploitation rather than to restrict exploration in dynamics-consistent OOD regions.

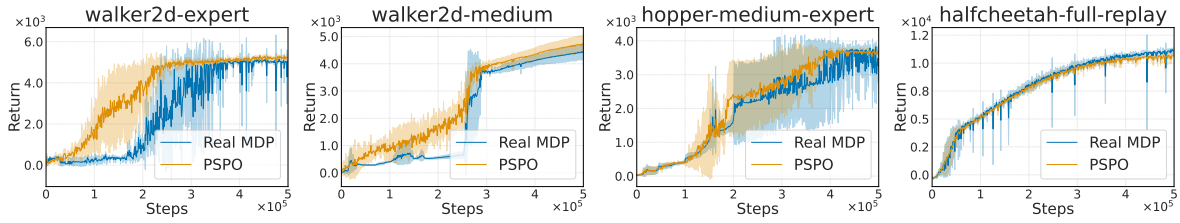


Figure 2: Learning and evaluation curves. We observe that the true performance improves near-monotonically, even though the returns estimated by the model exhibit no pessimism.

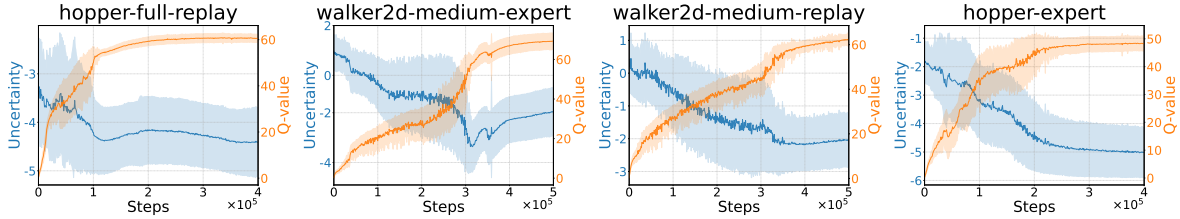


Figure 3: Correlation between uncertainty and the TD target. The target is defined as $Q(s, a) = r(s, a) + \gamma \mathbb{E}_{s' \sim T, a' \sim \pi} [Q(s', a')]$. Here, uncertainty for a pair (s, a) is quantified as $\log(\text{std}(\mathbb{E}_{s' \sim T}[s']))$ with $T \sim P(T|E)$.

Table 3: Ablation study results. We report the percentage drop in scores (\downarrow) and the fold change in standard deviation (\uparrow / \downarrow). The notation ‘x’ indicates the fold change (e.g., $\uparrow 9x$ represents a 9-fold increase). We observe that ablating either component leads to substantial performance degradation and a notable increase in standard deviation.

Dataset Type	Ablation Setting	HalfCheetah	Hopper	Walker2d
Random	Average Utilization	$\downarrow 19.1\%$ ($\uparrow 9x$)	$\downarrow 68.1\%$ ($\downarrow 0.5x$)	$\downarrow 14.5\%$ ($\uparrow 35x$)
	Without Regularization	$\downarrow 13.3\%$ ($\uparrow 1.7x$)	$\downarrow 68.1\%$ ($\uparrow 1.1x$)	$\downarrow 13.9\%$ ($\uparrow 53x$)
Medium	Average Utilization	$\downarrow 5.9\%$ ($\uparrow 2.2x$)	$\downarrow 68.1\%$ ($\downarrow 0.9x$)	$\downarrow 3.9\%$ ($\downarrow 0.96x$)
	Without Regularization	$\downarrow 5.8\%$ ($\uparrow 1.6x$)	$\downarrow 13.2\%$ ($\uparrow 9.5x$)	$\downarrow 9.1\%$ ($\uparrow 1.6x$)
Expert	Average Utilization	$\downarrow 11.2\%$ ($\uparrow 16x$)	$\downarrow 53.4\%$ ($\uparrow 4.4x$)	$\downarrow 67.1\%$ ($\uparrow 13.5x$)
	Without Regularization	$\downarrow 23.9\%$ ($\uparrow 4.4x$)	$\downarrow 20.0\%$ ($\uparrow 14.9x$)	$\downarrow 78.6\%$ ($\uparrow 2x$)
Medium-Expert	Average Utilization	$\downarrow 3.9\%$ ($\uparrow 3.1x$)	$\downarrow 9.9\%$ ($\uparrow 5.4x$)	$\downarrow 16.3\%$ ($\uparrow 12x$)
	Without Regularization	$\downarrow 17.3\%$ ($\uparrow 1.5x$)	$\downarrow 12.8\%$ ($\uparrow 8x$)	$\downarrow 8.3\%$ ($\uparrow 3.6x$)
Medium-Replay	Average Utilization	$\downarrow 9.4\%$ ($\uparrow 4x$)	$\downarrow 67.9\%$ ($\uparrow 1.3x$)	$\downarrow 1.7\%$ ($\uparrow 2.2x$)
	Without Regularization	$\downarrow 9.1\%$ ($\uparrow 2.1x$)	$\downarrow 4.7\%$ ($\uparrow 6.8x$)	$\downarrow 8.1\%$ ($\uparrow 1.1x$)
Full-Replay	Average Utilization	$\downarrow 5.6\%$ ($\uparrow 1.9x$)	$\downarrow 11.1\%$ ($\uparrow 6x$)	$\downarrow 4.8\%$ ($\uparrow 1.9x$)
	Without Regularization	$\downarrow 7.4\%$ ($\uparrow 1.6x$)	$\downarrow 10.3\%$ ($\uparrow 10.4x$)	$\downarrow 9.3\%$ ($\uparrow 1.5x$)

Robustness Figure 3 reveals a negative correlation (Spearman’s rank correlation $\tau = -0.2995$) between the TD target and our uncertainty metric. This confirms that model disagreement induces an adaptive posterior reweighting that mitigates overestimation. Rather than using indiscriminate pessimism, PSPO selectively penalizes state-action pairs that deviate from the data distribution to guide the policy back to dynamics-consistent regions, successfully balancing generalization with OOD robustness.

Generalization To assess performance under high uncertainty, we employ a currency liquidation environment in which an agent must liquidate assets over a fixed horizon T amid stochastic rate fluctuations. In this environment, the behavioral policy is heavily biased toward “hold” actions (80%). The underlying market dynamics follow

a coherent Ornstein-Uhlenbeck process (details in Appendix E.1.2). We benchmark PSPO against additional model-free (ORAAC [38], IQL [13]) and model-based (MOPO [43], COMBO [44]) methods. As summarized in Table 2, while existing methods struggle to converge in this highly stochastic setting, PSPO consistently achieves superior stability and higher cumulative returns. This performance indicates that PSPO extends beyond simple value suppression in OOD regions. By leveraging the posterior distribution to provide dynamically consistent estimates, PSPO facilitates safe extrapolation and effective generalization, preventing catastrophic failures during policy deviation while identifying superior decision sequences in adjacent state-action supports.

5.3 Ablation Study (Q3)

To isolate the impact of PSPO’s distinct components, we conduct an ablation study focusing on the posterior sampling mechanism (Eq. 3-Eq. 4) and the reference policy regularization (Eq. 7). For the posterior sampling component, we disable the reweighting process based on the evidence term $\mathcal{F}(T)$. Instead, we enforce a uniform posterior distribution over the dynamics models, designating this variant as “Average Utilization.” Regarding the regularization component, we exclude the reference policy μ entirely, referring to this variant as “Without Regularization.” As shown in Table 3, ablating either component significantly degrades performance and increases training instability, evidenced by a larger standard deviation.

6 Related Work

Offline RL Offline RL aims to learn optimal policies entirely from a fixed dataset of historical interactions, without further access to the environment [15]. The primary challenge in offline RL is distribution shift [3, 46]. In practice, this issue is typically mitigated by employing pessimistic approaches. In model-free offline RL, pessimism is realized either by explicitly penalizing the Q-values of OOD actions [14, 42, 11], or by implicitly assigning a low weight to them [13, 23]. In model-based offline RL, pessimism is commonly introduced by either constructing a dynamics model ensemble and using the predicted uncertainty (e.g., standard deviation) as a penalty [12, 43, 37, 31], or by formulating a two-player zero-sum game based on robust MDPs [33, 10, 6]. However, recent literature confirms a positive correlation between the generalization ability of offline RL and state-action space coverage, suggesting that pessimism may detrimentally affect generalization [24, 29]. Therefore, despite efforts to broaden coverage via optimistic sampling [45] or high-fidelity trajectory synthesis [17], these approaches still resort to uncertainty-based penalization to realize pessimism, limiting their ability to fully leverage model generalization.

We propose a novel model-based algorithm that treats the dynamics model as a random variable and maintains a corresponding distribution. Compared to prior methods, our approach explicitly avoids uncertainty-based penalization, leading to a theoretically non-pessimistic framework.

Bayesian RL Bayesian RL manages uncertainty by first constructing a posterior belief over an ensemble of dynamics models and subsequently optimizing a policy under this belief [39, 19, 28]. Existing Bayesian RL works diverge primarily in belief construction and policy optimization. For belief construction, existing methods either derive the posterior through Bayesian inference with an implicit likelihood or assume a fixed posterior directly induced by the offline dataset [33, 10, 6, 4]. As for policy optimization in Bayesian RL, methods typically introduce pessimism through risk-sensitive objectives, such as Conditional Value at Risk (CVaR) [21, 32], or ensure stability via regularized policy iteration [27, 10, 18]. In the context of offline Bayesian RL, the finite capacity of the dataset is typically insufficient to uniquely identify the true dynamics model [9]. While Bayesian RL offers a natural framework to quantify this epistemic uncertainty [4], prior works typically rely on pessimism by enforcing conservative constraints on belief formation or the optimization objective [33, 9, 34]. This dependence on pessimistic regularization inevitably limits the inherent adaptability of Bayesian RL.

Unlike prior works, PSPO imposes no structural assumptions on the posterior form and avoids pessimism. Our approach achieves generalization through posterior sampling, while ensuring robustness against OOD exploitation through the policy optimization process.

7 Conclusion

We present PSPO, a pessimism-free model-based offline RL framework that balances generalization with robustness against model exploitation. By synthesizing dynamics-consistent OOD transitions via posterior sampling and employing constrained optimization to regularize policy updates, PSPO effectively generalizes beyond the dataset support while maintaining stability. Theoretically, we formulate Q-value estimation under posterior sampling as a stochastic approximation process with guaranteed convergence. Furthermore, we prove that the policy optimization ensures monotonic performance gains until convergence. Experimental results demonstrate that PSPO achieves SoTA performance across diverse benchmarks. A promising direction involves utilizing generative modeling to learn data-driven informative priors, thereby reducing the reliance on manual specifications or standard uninformative priors. We anticipate that this integration will bolster the generalization of offline policies and facilitate more sample-efficient learning in high-dimension environments.

References

- [1] Wenhao Bao and Xiao-yang Liu. Multi-agent deep reinforcement learning for liquidation strategy analysis. *Arxiv*, 2019.
- [2] Pier Giovanni Bissiri, Chris C Holmes, and Stephen G Walker. A general framework for updating belief distributions. *Journal of the Royal Statistical Society Series B: Statistical Methodology*, 2016.
- [3] David Brandfonbrener, Will Whitney, Rajesh Ranganath, and Joan Bruna. Offline rl without off-policy evaluation. *Advances in neural information processing systems*, 2021.
- [4] Yunseon Choi, Li Zhao, Chuheng Zhang, Lei Song, Jiang Bian, and Kee-Eung Kim. Diversification of adaptive policy for effective offline reinforcement learning. In *Proceedings of the Thirty-Third International Joint Conference on Artificial Intelligence*, 2024.
- [5] Kurtland Chua, Roberto Calandra, Rowan McAllister, and Sergey Levine. Deep reinforcement learning in a handful of trials using probabilistic dynamics models. *Advances in neural information processing systems*, 2018.
- [6] Jing Dong, Jingwei Li, Baoxiang Wang, and Jingzhao Zhang. Online policy optimization for robust markov decision process. In *The 40th Conference on Uncertainty in Artificial Intelligence*, 2024.
- [7] Justin Fu, Aviral Kumar, Ofir Nachum, George Tucker, and Sergey Levine. D4rl: Datasets for deep data-driven reinforcement learning. *Arxiv*, 2020.
- [8] Mohammad Ghavamzadeh, Shie Mannor, Joelle Pineau, Aviv Tamar, et al. Bayesian reinforcement learning: A survey. *Foundations and Trends® in Machine Learning*, 2015.
- [9] Dibya Ghosh, Anurag Ajay, Pulkit Agrawal, and Sergey Levine. Offline rl policies should be trained to be adaptive. In *International Conference on Machine Learning*, 2022.
- [10] Kaiyang Guo, Shao Yunfeng, and Yanhui Geng. Model-based offline reinforcement learning with pessimism-modulated dynamics belief. *Advances in Neural Information Processing Systems*, 2022.
- [11] Longyang Huang, Botao Dong, and Weidong Zhang. Efficient offline reinforcement learning with relaxed conservatism. *IEEE Transactions on Pattern Analysis and Machine Intelligence*, 2024.
- [12] Rahul Kidambi, Aravind Rajeswaran, Praneeth Netrapalli, and Thorsten Joachims. Morel: Model-based offline reinforcement learning. *Advances in neural information processing systems*, 33:21810–21823, 2020.
- [13] Ilya Kostrikov, Ashvin Nair, and Sergey Levine. Offline reinforcement learning with implicit q-learning. In *Deep RL Workshop NeurIPS 2021*, 2021.
- [14] Aviral Kumar, Aurick Zhou, George Tucker, and Sergey Levine. Conservative q-learning for offline reinforcement learning. *Advances in neural information processing systems*, 2020.
- [15] Sergey Levine, Aviral Kumar, G. Tucker, and Justin Fu. Offline reinforcement learning: Tutorial, review, and perspectives on open problems. *ArXiv*, 2020.
- [16] Yuxuan Li, Yicheng Gao, Ning Yang, and Stephen Xia. Tw-crl: Time-weighted contrastive reward learning for efficient inverse reinforcement learning. In *Proceedings of the AAAI Conference on Artificial Intelligence*, 2026.
- [17] Haoxin Lin, Yu-Yan Xu, Yihao Sun, Zhilong Zhang, Yi-Chen Li, Chengxing Jia, Junyin Ye, Jiayi Zhang, and Yang Yu. Any-step dynamics model improves future predictions for online and offline reinforcement learning. In *International Conference on Learning Representations*, 2025.
- [18] Hongqiang Lin, Zhenghui Fu, Weihao Tang, Pengfei Wang, Yiding Sun, Qixian Huang, and Dongxu Zhang. Robust regularized policy iteration under transition uncertainty. *Arxiv*, 2026.
- [19] Qian Lin, Zongkai Liu, Danying Mo, and Chao Yu. An offline adaptation framework for constrained multi-objective reinforcement learning. In *Advances in Neural Information Processing Systems*, 2024.
- [20] Wenhui Liu, Zhijian Wu, Jingchao Wang, Dingjiang Huang, and Shuigeng Zhou. Imagination-limited q-learning for offline reinforcement learning. In *Proceedings of the Thirty-Fourth International Joint Conference on Artificial Intelligence*, 2025.

- [21] Elita A Lobo, Mohammad Ghavamzadeh, and Marek Petrik. Soft-robust algorithms for batch reinforcement learning. *Arxiv*, 2020.
- [22] Cong Lu, Philip Ball, Jack Parker-Holder, Michael Osborne, and Stephen J Roberts. Revisiting design choices in offline model based reinforcement learning. In *International Conference on Learning Representations*, 2022.
- [23] Yixiu Mao, Cheems Wang, Yun Qu, Yuhang Jiang, and Xiangyang Ji. Doubly mild generalization for offline reinforcement learning. In *Advances in neural information processing systems*, 2024.
- [24] Ishita Mediratta, Qingfei You, Minqi Jiang, and Roberta Raileanu. The generalization gap in offline reinforcement learning. In *International Conference on Learning Representations*, 2024.
- [25] Volodymyr Mnih, Koray Kavukcuoglu, David Silver, Andrei A Rusu, Joel Veness, Marc G Bellemare, Alex Graves, Martin Riedmiller, Andreas K Fidjeland, Georg Ostrovski, et al. Human-level control through deep reinforcement learning. *nature*, 2015.
- [26] Thomas M Moerland, Joost Broekens, Aske Plaat, Catholijn M Jonker, et al. Model-based reinforcement learning: A survey. *Foundations and Trends® in Machine Learning*, 2023.
- [27] Gergely Neu, Anders Jonsson, and Vicenç Gómez. A unified view of entropy-regularized markov decision processes, 2017.
- [28] Tianwei Ni, Esther Derman, Vineet Jain, Vincent Taboga, Siamak Ravanbakhsh, and Pierre-Luc Bacon. Long-horizon model-based offline reinforcement learning without conservatism. *Arxiv*, 2025.
- [29] Seohong Park, Kevin Frans, Sergey Levine, and Aviral Kumar. Is value learning really the main bottleneck in offline rl? *Advances in Neural Information Processing Systems*, 2024.
- [30] Seohong Park, Qiyang Li, and Sergey Levine. Flow q-learning. In *International Conference on Machine Learning*, 2025.
- [31] Zhongjian Qiao, Jiafei Lyu, Kechen Jiao, Qi Liu, and Xiu Li. Sumo: Search-based uncertainty estimation for model-based offline reinforcement learning. *Proceedings of the AAAI Conference on Artificial Intelligence*, 2025.
- [32] Marc Rigter, Paul Duckworth, Bruno Lacerda, and Nick Hawes. Planning for risk-aversion and expected value in mdps. In *Proceedings of the International Conference on Automated Planning and Scheduling*, 2022.
- [33] Marc Rigter, Bruno Lacerda, and Nick Hawes. Rambo-rl: Robust adversarial model-based offline reinforcement learning. *Advances in neural information processing systems*, 2022.
- [34] Marc Rigter, Bruno Lacerda, and Nick Hawes. One risk to rule them all: A risk-sensitive perspective on model-based offline reinforcement learning. *Advances in neural information processing systems*, 2023.
- [35] Herbert Robbins and Sutton Monro. A stochastic approximation method. *The annals of mathematical statistics*, pages 400–407, 1951.
- [36] John Schulman, Sergey Levine, Pieter Abbeel, Michael Jordan, and Philipp Moritz. Trust region policy optimization. In *International Conference on Machine Learning*, 2015.
- [37] Yihao Sun, Jiayi Zhang, Chengxing Jia, Haoxin Lin, Junyin Ye, and Yang Yu. Model-bellman inconsistency for model-based offline reinforcement learning. In *International Conference on Machine Learning*, 2023.
- [38] Núria Armengol Urpí, Sebastian Curi, and Andreas Krause. Risk-averse offline reinforcement learning. In *International Conference on Learning Representations*, 2021.
- [39] Ran Wei, Siliang Zeng, Chenliang Li, Alfredo Garcia, Anthony D McDonald, and Mingyi Hong. A bayesian approach to robust inverse reinforcement learning. In *Conference on Robot Learning*, 2023.
- [40] Ning Yang, Pengyu Wang, Guoqing Liu, Haifeng Zhang, Pin Lyu, and Jun Wang. Proactive constrained policy optimization with preemptive penalty. In *Proceedings of the AAAI Conference on Artificial Intelligence*, 2026.
- [41] Qianlan Yang and Yu-Xiong Wang. RTDiff: Reverse trajectory synthesis via diffusion for offline reinforcement learning. In *International Conference on Learning Representations*, 2025.
- [42] Junghyuk Yeom, Yonghyeon Jo, Jeongmo Kim, Sanghyeon Lee, and Seungyul Han. Exclusively penalized q-learning for offline reinforcement learning. *Advances in Neural Information Processing Systems*, 37:113405–113435, 2024.

- [43] Tianhe Yu, Garrett Thomas, Lantao Yu, Stefano Ermon, James Y Zou, Sergey Levine, Chelsea Finn, and Tengyu Ma. Mopo: Model-based offline policy optimization. *Advances in Neural Information Processing Systems*, 2020.
- [44] Tianhe Yu, Aviral Kumar, Rafael Rafailov, Aravind Rajeswaran, Sergey Levine, and Chelsea Finn. Combo: Conservative offline model-based policy optimization. *Advances in neural information processing systems*, 2021.
- [45] Y Zhai, Y Li, Z Gao, et al. Optimistic model rollouts for pessimistic offline policy optimization. In *Proceedings of the AAAI Conference on Artificial Intelligence*, 2024.
- [46] Zhe Zhang and Xiaoyang Tan. Adaptive reward shifting based on behavior proximity for offline reinforcement learning. In *Proceedings of the Thirty-Second International Joint Conference on Artificial Intelligence*, 2023.

Appendix

A Basic Knowledge about Bayesian RL

We begin by reviewing the formal framework of Bayesian Reinforcement Learning (BRL), which offers a rigorous method for handling uncertainty in decision-making. We then discuss how these principles are pragmatically adapted in modern Model-Based Deep Reinforcement Learning (MBRL) through the use of deep ensembles and trajectory sampling.

A.1 Standard Bayesian Reinforcement Learning

The standard RL problem is modeled as a Markov Decision Process (MDP), defined by the tuple $\mathcal{M} = \langle \mathcal{S}, \mathcal{A}, T, R, \gamma \rangle$. In the classical frequentist view, the transition dynamics $T(s'|s, a)$ and reward function $R(s, a)$ are assumed to be fixed but unknown parameters. Bayesian RL, in contrast, treats these unknown parameters as random variables. It maintains a prior distribution $P(\theta)$ over the model parameters $\theta = \{T, R\}$, quantifying the agent’s subjective uncertainty about the environment.

A.1.1 Inference and Belief State

As the agent interacts with the environment and collects a history of transitions $\mathcal{D}_t = \{(s_i, a_i, r_i, s'_i)\}_{i=0}^t$, it updates its posterior distribution over the parameters using Bayes’ rule:

$$P(\theta|\mathcal{D}_t) \propto P(\mathcal{D}_t|\theta)P(\theta).$$

This posterior distribution represents the agent’s current knowledge. For discrete MDPs, conjugate priors such as the Dirichlet distribution for transition probabilities and the Gamma-Normal pair for rewards are commonly employed to maintain the posterior within the same family while ensuring computational tractability.

To formalize the temporal evolution of this knowledge, we define the belief transition as a recursive Bayesian filtering process. Let $b_t(\theta)$ denote the probability density function over the parameters at time step t . Then, for $b_{t+1}(\theta) = P(\theta|\mathcal{D}_{t+1})$, we have:

$$\begin{aligned} b_{t+1}(\theta) &= P(\theta|\mathcal{D}_{t+1}) \\ &= P(\theta|s', r, s, a, \mathcal{D}_t) \\ &= \frac{\overbrace{P(s', r|s, a, \mathcal{D}_t, \theta)}^{\text{Likelihood}} \cdot \overbrace{P(\theta|s, a, \mathcal{D}_t)}^{\text{Prior}}}{\underbrace{P(s', r|s, a, \mathcal{D}_t)}_{\text{Normalization Term}}}. \end{aligned}$$

Invoking the Markov property, the transition dynamics are independent of the history \mathcal{D}_t given the current state, action, and parameters: $P(s', r|s, a, \mathcal{D}_t, \theta) = P(s', r|s, a, \theta)$. Furthermore, given \mathcal{D}_t , the parameter θ is conditionally independent of the current state-action pair (s, a) , as (s, a) reveals no information about θ before the transition is observed. Consequently, we have $P(\theta|s, a, \mathcal{D}_t) = P(\theta|\mathcal{D}_t) := b_t(\theta)$. Applying Bayes’ rule yields the update:

$$b_{t+1}(\theta) = \eta \cdot \underbrace{P(s', r|s, a, \theta)}_{\text{Likelihood}} \cdot \underbrace{b_t(\theta)}_{\text{Prior}},$$

where η is the normalization constant.

A.1.2 The Bayes-Adaptive MDP (BAMDP)

Formally, the BRL problem is cast as finding the optimal policy within a Bayes-Adaptive MDP (BAMDP), denoted as the tuple $\mathcal{M}^+ = \langle \mathcal{S}^+, \mathcal{A}, T^+, R^+, \gamma \rangle$. In this augmented framework, the state space $\mathcal{S}^+ = \mathcal{S} \times \mathcal{B}$ concatenates the physical state s with the belief state $b(\theta) = P(\theta|\mathcal{D}_t)$, which represents the posterior distribution over the unknown system parameters θ (i.e., transition dynamics and reward functions). The transition dynamics in the hyper-state are governed by T^+ , which defines the evolution $(s, b) \rightarrow (s', b')$. Specifically, the probability of such a transition is quantified by the predictive distribution $P(s'|s, b, a)$. The probability of transitioning to a physical state s' given the current hyper-state (s, b) and action a is obtained by marginalizing over the parameter space Θ :

$$P(s'|s, b, a) = \int_{\Theta} T(s'|s, a; \theta)b(\theta)d\theta.$$

Crucially, the belief state evolves deterministically. Upon observing a transition (s, a, s') , the belief updates via Bayes' rule, $b' = \Psi(b, s, a, s')$, where Ψ is the Bayesian update operator. The objective of the agent is to maximize the expected cumulative reward with respect to its belief. This is encapsulated by the Bellman optimality equation for BAMDPs:

$$V^*(s, b) = \max_{a \in \mathcal{A}} \left[R(s, a) + \gamma \sum_{s' \in \mathcal{S}} P(s'|s, b, a)V^*(s', \Psi(b, s, a, s')) \right].$$

This formulation naturally resolves the exploration-exploitation dilemma. The optimal value function $V^*(s, b)$ encodes an implicit incentive mechanism that prioritizes actions leading to belief states b' with reduced entropy (equivalent to maximizing information gain). This systematic preference for uncertainty reduction inherently drives the agent to explore uncharted regions of the state space, thereby improving the precision of its internal model estimates. However, exact planning via the Bellman equation is computationally intractable for most non-trivial problems due to the continuous and high-dimensional nature of the belief space \mathcal{B} . To circumvent this intractability, BRL algorithms frequently employ sampling-based approximations. A prominent example is Thompson Sampling (TS). Instead of maximizing the expectation over the full posterior predictive distribution $P(s'|s, b, a)$, TS samples a single hypothesis $\hat{\theta} \sim b_t(\theta)$ at each step (or episode) and selects the action that is optimal with respect to this sampled model:

$$a_t = \arg \max_{a \in \mathcal{A}} Q^*(s, a; \hat{\theta}).$$

This heuristic effectively converts the complex Bayesian planning problem into a standard MDP planning problem, relying on the variance of the posterior b_t to drive stochastic exploration.

A.2 Modern Approximation: Deep Ensembles in Model-Based RL

In high-dimensional environments (e.g., robotics or visual tasks), the dynamics are modeled using Deep Neural Networks (DNNs), parameterized by weights \mathbf{w} . The posterior distribution over network weights $P(\mathbf{w}|\mathcal{D})$ lies on a complex manifold in a high-dimensional space, rendering exact Bayesian inference and conjugate updates impossible.

A.2.1 Deep Ensembles as Approximate Posteriors

To bridge the gap between BRL theory and Deep RL scalability, modern approaches typically employ Deep Ensembles (or Bootstrapped Ensembles) to approximate the posterior. An ensemble of K probabilistic neural networks, $\{\psi_{\mathbf{w}_k}\}_{k=1}^K$, is trained on the collected data. Each network outputs a distribution over the next state (e.g., a Gaussian $\mathcal{N}(\mu_{\mathbf{w}}(s, a), \Sigma_{\mathbf{w}}(s, a))$) to capture aleatoric uncertainty (inherent stochasticity). Crucially, the set of networks serves as a non-parametric approximation of the posterior over the function space. The variance of predictions across the ensemble members quantifies the epistemic uncertainty. This aligns with the BRL philosophy: regions of the state space with sparse data will induce high disagreement among ensemble members (high posterior variance), thereby encouraging exploration.

A.2.2 Trajectory Sampling (TS)

To perform planning with these ensembles, methods such as Probabilistic Ensembles with Trajectory Sampling (PETS) implement the principle of Thompson Sampling within a Model Predictive Control (MPC) framework [5]. Instead of averaging the predictions of the ensemble models (which would collapse the uncertainty), Trajectory Sampling maintains specific particles during imaginary rollouts. For each particle, a specific ensemble member (a hypothesis of the world dynamics) is sampled and fixed for the duration of the rollout. This process mimics sampling a transition function $\hat{T} \sim P(T|\mathcal{D})$ in classical BRL, allowing the agent to perform consistent reasoning under uncertainty. By selecting actions that maximize expected returns over these sampled trajectories, the agent naturally balances exploration and exploitation, consistent with the theoretical guarantees of Bayesian RL.

A.3 PSPO (Our Method)

Following established paradigms, PSPO employs an ensemble of probabilistic neural networks to model transition dynamics, maintaining a belief distribution that rigorously quantifies epistemic uncertainty. Crucially, our approach leverages the Principle of Minimum Information to derive a posterior conditioned on empirical evidence, explicitly circumventing the restrictive fixed posterior assumption. For rollout generation, PSPO samples models directly from this adaptive belief, aligning with classic Bayesian RL to facilitate controlled exploration. Building on this, we formulate a policy optimization framework that decomposes the constrained objective into a sequence of tractable subproblems, providing theoretical guarantees for monotonic improvement. Collectively, PSPO effectively strikes a balance between generalization capability and OOD robustness.

B Other prerequisite knowledge

B.1 Regularized Optimization

We need to solve the following regularized optimization problem to find the optimal policy π :

$$\begin{aligned} \min_{\pi} & \left\{ \sum_a \pi(a|s)q(s, a) - \lambda \mathcal{H}(\pi(a|s)) \right\}, \\ \text{s.t.} & \sum_a \pi(a|s) = 1, \\ & \pi(a|s) \geq 0, \end{aligned}$$

where the Shannon entropy $\mathcal{H}(\pi(a|s)) = -\sum_a \pi(a|s) \log(\pi(a|s))$. Substituting this into the objective function, the original problem is equivalent to:

$$\min_{\pi} \left\{ \sum_a \pi(a|s)q(s, a) + \lambda \pi(a|s) \log(\pi(a|s)) \right\},$$

The Lagrangian function $\mathcal{L}(\tilde{\alpha}, z, \tilde{\mu})$ is constructed as follows:

$$\begin{aligned} \mathcal{L}(\pi, z, \mu) &= \sum_a \pi(a|s)q(s, a) + \lambda \sum_a \pi(a|s) \log(\pi(a|s)) \\ &\quad - z \left(\sum_a \pi(a|s) - 1 \right) - \sum_a \mu \pi(a|s). \end{aligned}$$

Here, z is the Lagrange multiplier corresponding to the equality constraint $\sum_a \pi(a|s) = 1$, and μ are the Lagrange multipliers corresponding to the inequality constraints $\pi(a|s) \geq 0$.

Due to the presence of the entropy term $\log(\pi(a|s))$, the optimal solution must lie in the interior of the probability simplex, i.e., $\pi(a|s) > 0$. According to the complementary slackness condition $\mu\pi(a|s) = 0$, when $\pi(a|s) > 0$, we must have $\mu = 0$. Under this condition, the stationarity condition simplifies to:

$$q(s, a) + \lambda(\log(\pi(a|s)) + 1) - z = 0.$$

The solution $\pi^*(a|s)$ is determined by solving the equation:

$$\begin{aligned} \lambda \log(\pi(a|s)) &= z - \lambda - q(s, a), \\ \log(\pi(a|s)) &= \frac{z - \lambda}{\lambda} - \frac{q(s, a)}{\lambda}, \\ \pi(a|s) &= \exp\left(\frac{z - \lambda}{\lambda} - \frac{q(s, a)}{\lambda}\right) \\ &= \exp\left(\frac{z - \lambda}{\lambda}\right) \cdot \exp\left(-\frac{q(s, a)}{\lambda}\right). \end{aligned}$$

Since $\exp\left(\frac{z - \lambda}{\lambda}\right)$ is a constant that does not depend on the index i , we can conclude that:

$$\pi^*(a|s) \propto \exp\left(-\frac{1}{\lambda}q(s, a)\right).$$

Let $\pi^*(a|s) = C \cdot \exp\left(-\frac{1}{\lambda}q(s, a)\right)$, then:

$$C = \frac{1}{\sum_a \exp\left(-\frac{1}{\lambda}q(s, a)\right)}.$$

Substituting the constant C back into the expression yields the final form of the optimal solution:

$$\pi^*(a|s) = \frac{\exp\left(-\frac{1}{\lambda}q(s, a)\right)}{\sum_a \exp\left(-\frac{1}{\lambda}q(s, a)\right)}.$$

By substituting the optimal solution $\pi^*(a|s) \propto \exp\left(-\frac{1}{\lambda}q(s, a)\right)$ into the primal problem, the resulting optimal value is given by:

$$-\lambda \log\left(\sum_a \exp\left(-\frac{q(s, a)}{\lambda}\right)\right).$$

C Notations

Objective function:

$$\mathcal{J}(\pi) = \mathbb{E}_{T_0 \sim P(T|\mathcal{D})}^{\rho_0, \pi} \left[\mathbb{E}_{T_1 \sim P(T|\mathcal{D})}^{\rho_0, \pi} \left[\cdots \mathbb{E}_{T_\infty, \pi}^{\rho_0, \pi} \left[\sum_{t=0}^{\infty} \gamma^t r(s_t, a_t) \right] \right] \right]. \quad (10)$$

Regularized objective function:

$$\tilde{\mathcal{J}}(\pi) = \mathbb{E}_{T_0 \sim P(T|\mathcal{D})}^{\rho_0, \pi} \left[\mathbb{E}_{T_1 \sim P(T|\mathcal{D})}^{\rho_0, \pi} \left[\cdots \mathbb{E}_{T_\infty, \pi}^{\rho_0, \pi} \left[\sum_{t=0}^{\infty} \gamma^t (r(s_t, a_t) - \alpha D_{\text{KL}}(\pi(\cdot|s_t) || \mu(\cdot|s_t))) \right] \right] \right]. \quad (11)$$

Posterior sampling-based Bellman operator:

$$(\bar{\mathcal{B}}^\pi Q)(s, a) = r(s, a) + \gamma \mathbb{E}_{\substack{T \sim P(T|E) \\ s' \sim T, a' \sim \pi}} [Q(s', a')]. \quad (12)$$

Posterior sampling-based Bellman optimality operator:

$$(\bar{\mathcal{B}}^* Q)(s, a) = r(s, a) + \gamma \mathbb{E}_{\substack{T \sim P(T|\mathcal{D}) \\ s' \sim T}} \left[\alpha \log \mathbb{E}_\mu \exp \left(\frac{Q(s', a')}{\alpha} \right) \right]. \quad (13)$$

Constrained optimization problem:

$$\begin{aligned} \pi_{i+1} &= \arg \max_{\pi} \tilde{\mathcal{J}}(\pi), \\ \text{s.t.} \quad & D_{\text{KL}}(\pi \| \pi_i) \leq \epsilon. \end{aligned} \quad (14)$$

D Proofs

Proposition 1. *The posterior sampling-based Bellman operator $\bar{\mathcal{B}}^\pi$ is a γ -contraction with respect to the L_∞ -norm.*

proof of Proposition 1. Let Q_1 and Q_2 be two arbitrary Q-functions. Then, considering the operator defined in Eq. (12):

$$\begin{aligned} & \|\bar{\mathcal{B}}^\pi Q_1 - \bar{\mathcal{B}}^\pi Q_2\|_\infty \\ &= \max_{s,a} |(\bar{\mathcal{B}}^\pi Q_1)(s, a) - (\bar{\mathcal{B}}^\pi Q_2)(s, a)| \\ &= \max_{s,a} \left| \left(r(s, a) + \gamma \mathbb{E}_{\substack{T \sim P(T|E) \\ s' \sim T, a' \sim \pi}} [Q_1(s', a')] \right) - \left(r(s, a) + \gamma \mathbb{E}_{\substack{T \sim P(T|E) \\ s' \sim T, a' \sim \pi}} [Q_2(s', a')] \right) \right| \\ &= \gamma \max_{s,a} \left| \mathbb{E}_{\substack{T \sim P(T|E) \\ s' \sim T, a' \sim \pi}} [Q_1(s', a') - Q_2(s', a')] \right| \\ &\leq \gamma \max_{s,a} \mathbb{E}_{\substack{T \sim P(T|E) \\ s' \sim T, a' \sim \pi}} [|Q_1(s', a') - Q_2(s', a')|] \\ &\leq \gamma \max_{s,a} \mathbb{E}_{\substack{T \sim P(T|E) \\ s' \sim T, a' \sim \pi}} [\|Q_1 - Q_2\|_\infty] \\ &= \gamma \|Q_1 - Q_2\|_\infty. \end{aligned}$$

Thus, $\bar{\mathcal{B}}^\pi$ is a γ -contraction with respect to the L_∞ -norm. \square

Proposition 2. *Assuming the reward is bounded such that $|r| \leq R_{\max}$, and let $Y_t(s, a)$ be the stochastic target computed at update t : $Y_t = r(s, a) + \gamma \mathbb{E}_{s' \sim T'(\cdot|s,a)} [V_t(s')]$ where $T' \sim P(T|\mathcal{D})$ and $V_t(s') = \mathbb{E}_{a' \sim \pi_t} [Q_t(s', a')]$. Then, the variance of Y_t satisfies $\text{Var}(Y_t) \leq \frac{R_{\max}^2}{(1-\gamma)^2}$.*

proof of Proposition 2. We start with the standard assumptions: $|r| \leq R_{\max}$ and $|V_t(s)| \leq \frac{R_{\max}}{1-\gamma}$, $|Q_t(s, a)| \leq \frac{R_{\max}}{1-\gamma}$. The maximum value of Y_t is bounded by:

$$\max(Y_t) \leq R_{\max} + \gamma \left(\frac{R_{\max}}{1-\gamma} \right) = \frac{R_{\max}(1-\gamma) + \gamma R_{\max}}{1-\gamma} = \frac{R_{\max}}{1-\gamma}.$$

The minimum value of Y_t is bounded by:

$$\min(Y_t) \geq -R_{\max} + \gamma \left(-\frac{R_{\max}}{1-\gamma} \right) = \frac{-R_{\max}(1-\gamma) - \gamma R_{\max}}{1-\gamma} = -\frac{R_{\max}}{1-\gamma}.$$

Since all possible realizations of the random variable Y_t are contained within the interval $[-\frac{R_{\max}}{1-\gamma}, \frac{R_{\max}}{1-\gamma}]$, we can apply Popoviciu's inequality for bounded random variables, which states that $\text{Var}(X) \leq \frac{(b-a)^2}{4}$ for $X \in [a, b]$. The variance of Y_t is then bounded as:

$$\text{Var}(Y_t) \leq \frac{1}{4} \left(\frac{R_{\max}}{1-\gamma} - \left(-\frac{R_{\max}}{1-\gamma} \right) \right)^2 = \frac{1}{4} \left(\frac{2R_{\max}}{1-\gamma} \right)^2 = \frac{4R_{\max}^2}{(1-\gamma)^2 \cdot 4} = \frac{R_{\max}^2}{(1-\gamma)^2}.$$

Thus, the variance of the stochastic update target Y_t is uniformly bounded. \square

Lemma 1. Let $V_Q(s) = \alpha \log \mathbb{E}_{a' \sim \mu} \exp \left(\frac{Q(s, a')}{\alpha} \right)$. For any Q -functions Q_1 and Q_2 , the following inequality holds:

$$\|V_{Q_1} - V_{Q_2}\|_{\infty} \leq \|Q_1 - Q_2\|_{\infty}.$$

proof of Lemma 1. Let $d = \|Q_1 - Q_2\|_{\infty}$. Then, we have:

$$Q_1(s, a) \leq Q_2(s, a) + d, \quad \forall s, a.$$

We then have $V_{Q_1}(s) - V_{Q_2}(s) \leq d$. The proof follows.

$$\begin{aligned} V_{Q_1}(s) &= \alpha \log \mathbb{E}_{a' \sim \mu} \exp \left(\frac{Q_1(s, a')}{\alpha} \right) \\ &\leq \alpha \log \mathbb{E}_{a' \sim \mu} \exp \left(\frac{Q_2(s, a') + d}{\alpha} \right) \\ &= \alpha \log \mathbb{E}_{a' \sim \mu} \left[\exp \left(\frac{Q_2(s, a')}{\alpha} \right) \cdot \exp \left(\frac{d}{\alpha} \right) \right] \\ &= \alpha \log \left[\exp \left(\frac{d}{\alpha} \right) \cdot \mathbb{E}_{a' \sim \mu} \exp \left(\frac{Q_2(s, a')}{\alpha} \right) \right] \\ &= \alpha \left[\log \left(\exp \left(\frac{d}{\alpha} \right) \right) + \log \mathbb{E}_{a' \sim \mu} \exp \left(\frac{Q_2(s, a')}{\alpha} \right) \right] \\ &= \alpha \left[\frac{d}{\alpha} + \frac{1}{\alpha} V_{Q_2}(s) \right] \\ &= d + V_{Q_2}(s). \end{aligned}$$

Similarly, assuming $Q_2(s, a) \leq Q_1(s, a) + d$, we can likewise obtain $V_{Q_2}(s) - V_{Q_1}(s) \leq d$. Combining these two inequalities implies that $|V_{Q_1}(s) - V_{Q_2}(s)| \leq d = \|Q_1 - Q_2\|_{\infty}$. Since this inequality holds for all s , taking the supremum over s yields $\|V_{Q_1} - V_{Q_2}\|_{\infty} \leq \|Q_1 - Q_2\|_{\infty}$. \square

Theorem 1. Starting from any function $Q : \mathcal{S} \times \mathcal{A} \rightarrow \mathbb{R}$ and iteratively applying posterior distribution-based Bellman optimality operator $\bar{\mathcal{B}}^*$, the resulting sequence converges to \bar{Q}^* . The optimal policy for the objective $\tilde{\mathcal{J}}(\pi)$ is then obtained from this fixed point as: $\pi^*(a|s) \propto \mu(a|s) \exp \left(\frac{1}{\alpha} \bar{Q}^*(s, a) \right)$.

proof of Theorem 1. For any Q -functions Q_1 and Q_2 , we have:

$$\|\bar{\mathcal{B}}^* Q_1 - \bar{\mathcal{B}}^* Q_2\|_{\infty} = \sup_{s, a} \left| (\bar{\mathcal{B}}^* Q_1)(s, a) - (\bar{\mathcal{B}}^* Q_2)(s, a) \right|.$$

Let $V_Q(s) = \alpha \log \mathbb{E}_{a' \sim \mu} \exp\left(\frac{Q(s, a')}{\alpha}\right)$. Then

$$\begin{aligned} |(\bar{\mathcal{B}}^* Q_1)(s, a) - (\bar{\mathcal{B}}^* Q_2)(s, a)| &= |(r(s, a) + \gamma \mathbb{E}_{T, s'} [V_{Q_1}(s')]) - (r(s, a) + \gamma \mathbb{E}_{T, s'} [V_{Q_2}(s')])| \\ &= |\gamma (\mathbb{E}_{T, s'} [V_{Q_1}(s')] - \mathbb{E}_{T, s'} [V_{Q_2}(s')])| \\ &= \gamma |\mathbb{E}_{T, s'} [V_{Q_1}(s') - V_{Q_2}(s')]| \\ &\leq \gamma \mathbb{E}_{T, s'} [|V_{Q_1}(s') - V_{Q_2}(s')|]. \end{aligned}$$

According to Lemma 1, we have

$$\begin{aligned} |(\bar{\mathcal{B}}^* Q_1)(s, a) - (\bar{\mathcal{B}}^* Q_2)(s, a)| &\leq \gamma \mathbb{E}_{T, s'} [\|Q_1 - Q_2\|_\infty] \\ &= \gamma \|Q_1 - Q_2\|_\infty. \end{aligned}$$

This implies that

$$\|\bar{\mathcal{B}}^* Q_1 - \bar{\mathcal{B}}^* Q_2\|_\infty \leq \gamma \|Q_1 - Q_2\|_\infty.$$

By the Banach Fixed-Point Theorem, this operator admits a unique fixed point \bar{Q}^* in the complete metric space of bounded functions, and repeated application of the operator converges to \bar{Q}^* .

According to definition of fixed point, we have:

$$\bar{Q}^*(s, a) = (\bar{\mathcal{B}}^* \bar{Q}^*)(s, a) = r(s, a) + \gamma \mathbb{E}_{T, s'} [V_{\bar{Q}^*}(s')].$$

Specifically, $V_Q(s)$ is the optimal value of the following optimization problem:

$$V_Q(s) = \max_{\pi(\cdot|s)} \left\{ \mathbb{E}_{a \sim \pi(\cdot|s)} [Q(s, a)] - \alpha D_{\text{KL}}(\pi(\cdot|s) \|\mu(\cdot|s)) \right\}.$$

Here, $D_{\text{KL}}(\pi \|\mu) = \sum_a \pi(a|s) \log\left(\frac{\pi(a|s)}{\mu(a|s)}\right)$ denotes the Kullback-Leibler (KL) divergence. The optimal policy π^* , by definition, is the strategy that achieves the maximum of the objective at the fixed point \bar{Q}^* . Then. We seek to solve:

$$\pi^*(\cdot|s) = \arg \max_{\pi} \left\{ \sum_a \pi(a|s) \bar{Q}^*(s, a) - \alpha D_{\text{KL}}(\pi(\cdot|s) \|\mu(\cdot|s)) \right\}.$$

This is a convex optimization problem subject to the constraint $\sum_a \pi(a|s) = 1$. We utilize the Lagrange multiplier method. Let \mathcal{L} be the Lagrangian (omitting s and a dependence for clarity):

$$\mathcal{L}(\pi, z) = \sum_a \pi(a) \bar{Q}^*(a) - \alpha \sum_a \pi(a) (\log \pi(a) - \log \mu(a)) - z \left(\sum_a \pi(a) - 1 \right).$$

We take the derivative with respect to $\pi(a)$ and set it to zero:

$$\frac{\partial \mathcal{L}}{\partial \pi(a)} = \bar{Q}^*(a) - \alpha ((\log \pi(a) + 1) - \log \mu(a)) - z = 0.$$

Rearranging the equation to solve for $\pi(a)$ yields:

$$\alpha \log \pi(a) = \bar{Q}^*(a) + \alpha \log \mu(a) - (\alpha + z).$$

Exponentiating both sides and simplifying:

$$\pi(a) = \exp\left(\frac{1}{\alpha} \bar{Q}^*(a) + \log \mu(a) - \frac{\alpha + z}{\alpha}\right).$$

This further simplifies to:

$$\pi(a) = \mu(a) \exp\left(\frac{\bar{Q}^*(a)}{\alpha}\right) \cdot C(z),$$

where $C(z) = \exp\left(-\frac{\alpha+z}{\alpha}\right)$ is a term independent of a that serves as the normalization constant. Consequently, the optimal policy takes the following unnormalized form:

$$\pi^*(a|s) \propto \mu(a|s) \exp\left(\frac{1}{\alpha}\bar{Q}^*(s, a)\right).$$

□

Theorem 2. Let $C_{\text{KL}}(\pi) = \mathcal{J}(\pi) - \tilde{\mathcal{J}}(\pi)$ denote the regularization term, and let $F = F(\pi_i)$ be the Fisher Information Matrix at π_i . If ϵ is sufficiently small and the condition $\|\nabla\mathcal{J}(\pi_i)\|_F^2 > \langle \nabla\mathcal{J}(\pi_i), \nabla C_{\text{KL}}(\pi_i) \rangle_F$ holds, then starting from an arbitrary policy π_0 , the sequence of policies $\{\pi_i\}_{i \geq 0}$ generated by iteratively solving Eq. (14) guarantees monotonic improvement of $\mathcal{J}(\pi)$, such that $\mathcal{J}(\pi_{i+1}) \geq \mathcal{J}(\pi_i)$.

proof of Theorem 2. According to definition:

$$C_{\text{KL}}(\pi) = \mathbb{E}_{\substack{\rho_0, \pi \\ T_0 \sim P(T|\mathcal{D})}} \left[\mathbb{E}_{\substack{T_0, \pi \\ T_1 \sim P(T|\mathcal{D})}} \left[\cdots \mathbb{E}_{T_\infty, \pi} \left[\sum_{t=0}^{\infty} \alpha D_{\text{KL}}(\pi(\cdot|s_t) || \mu(\cdot|s_t)) \right] \right] \right],$$

where $\mu(\cdot|s_t)$ denotes the behavior policy used to collect the offline dataset. We consider the Lagrangian function $L(\pi, \lambda)$:

$$L(\pi, \lambda) = \tilde{\mathcal{J}}(\pi) - \lambda(D_{\text{KL}}(\pi || \pi_i) - \epsilon),$$

where $\lambda \geq 0$ is the Lagrange multiplier. At the optimal solution π_{i+1} , the stationarity condition must hold:

$$\nabla \tilde{\mathcal{J}}(\pi_{i+1}) = \lambda^* \nabla D_{\text{KL}}(\pi_{i+1} || \pi_i).$$

When ϵ is sufficiently small, we can Taylor-expand the KL divergence $D_{\text{KL}}(\pi || \pi_i)$ around $\pi = \pi_i$:

$$D_{\text{KL}}(\pi || \pi_i) \approx D_{\text{KL}}(\pi_i || \pi_i) + \nabla D_{\text{KL}}|_{\pi_i}(\pi - \pi_i) + \frac{1}{2}(\pi - \pi_i)^T \nabla^2 D_{\text{KL}}|_{\pi_i}(\pi - \pi_i),$$

where $\nabla^2 D_{\text{KL}}|_{\pi_i} = F(\pi_i)$ is the Fisher Information Matrix. Consequently, the gradient of the KL divergence at π_{i+1} can be approximated as:

$$\nabla D_{\text{KL}}(\pi_{i+1} || \pi_i) \approx F(\pi_i)(\pi_{i+1} - \pi_i) = F(\pi_i)v,$$

where $v = \pi_{i+1} - \pi_i$ denote the update direction. By the continuity of the gradient (i.e., $\nabla \tilde{\mathcal{J}}(\pi_{i+1}) \approx \nabla \tilde{\mathcal{J}}(\pi_i)$), we obtain:

$$v \approx (\lambda^*)^{-1} F(\pi_i)^{-1} \nabla \tilde{\mathcal{J}}(\pi_i).$$

We need to prove that:

$$\nabla \mathcal{J}(\pi_i)^T v \geq 0.$$

We have

$$\begin{aligned} \nabla \mathcal{J}(\pi_i)^T v &= (\lambda^*)^{-1} \nabla \mathcal{J}(\pi_i)^T F(\pi_i)^{-1} (\nabla \mathcal{J}(\pi_i) - \nabla C_{\text{KL}}(\pi_i)) \\ &= (\lambda^*)^{-1} \|\nabla \mathcal{J}(\pi_i)\|_F^2 - \langle \nabla \mathcal{J}(\pi_i), \nabla C_{\text{KL}}(\pi_i) \rangle_F \\ &\geq 0. \end{aligned}$$

□

E Experimental Details

E.1 Dataset

E.1.1 D4RL

To comprehensively assess performance across diverse offline scenarios, our experimental assessment encompasses a comprehensive benchmark spanning eighteen distinct experimental settings. These domains arise from the combination of three continuous control tasks (hopper, walker2d, and halfcheetah) with six diverse offline datasets that vary in quality and collection strategy.

- **Random:** A dataset generated by a randomly initialized policy. This setting represents the most challenging scenario with low-quality data and high entropy, testing the algorithm’s ability to extract meaningful learning signals from noisy interactions without any expert guidance.
- **Expert:** A dataset collected by a fully converged Soft Actor-Critic (SAC) agent. This dataset consists of high-return trajectories but covers a relatively narrow region of the state-action space. It evaluates the algorithm’s capacity for imitation and its ability to avoid overfitting to a deterministic behavior policy.
- **Medium:** A dataset generated by a policy trained to approximately one-third of the expert’s performance. This represents a competent but suboptimal baseline, challenging the algorithm to extrapolate beyond the demonstrated performance to achieve optimality.
- **Medium-Expert:** A composite dataset constructed by mixing equal parts (50-50 split) of medium and expert trajectories. This setting introduces a multimodal data distribution with mixed quality, requiring the algorithm to effectively distinguish between optimal and suboptimal transitions and selectively leverage high-reward data while ignoring inferior samples.
- **Medium-Replay:** A dataset comprising the entire replay buffer recorded during the training of the medium policy. Unlike the fixed medium dataset, this captures the full evolution of the agent from random initialization to intermediate competence, offering high state-space coverage but significant variance in transition quality.
- **Full-Replay:** This dataset encompasses the complete spectrum of policy evolution, ranging from random exploration to convergence. It offers the highest information density but also presents a challenge due to the extensive diversity and scale of the data.

E.1.2 Optimal Liquidation

This benchmark is an adaptation of the Optimal Liquidation Problem for offline RL, adhering to the protocol established by [34]. The primary objective is to maximize the realized revenue obtained from liquidating an initial inventory of 100 units of a specific asset (Currency A) into a target asset (Currency B) within a finite time horizon T , governed by stochastically evolving market dynamics. At every time step, the agent serves as an execution algorithm that must determine the optimal liquidation schedule, specifically deciding the proportion of the remaining inventory to execute.

This formulation presents a fundamental sequential decision-making challenge characterized by the tension between market risk and potential return. At each decision point, the agent must strategically balance the incentive to delay execution, which offers the possibility of capturing favorable price movements, against the substantial risk of adverse market shifts that could significantly erode the asset’s value. Consequently, the optimal policy must transcend simple heuristics to navigate a complex landscape of price uncertainty. It requires distinguishing between conservative strategies, such as immediate liquidation or uniform execution (akin to Time-Weighted Average Price strategies) which prioritize variance reduction, and aggressive strategies that hold inventory in anticipation of price recovery despite the exposure to heightened volatility.

Formulation: The liquidation environment is mathematically formulated as a finite-horizon Markov Decision Process. The state space is characterized by a three-dimensional vector $s_t = (t, m_t, p_t)$, encompassing the current discrete time step $t \in \{0, 1, \dots, T\}$, the remaining inventory of Currency A denoted by $m_t \in [0, 100]$, and the instantaneous exchange rate $p_t \in [0, \infty)$. The episode initializes with an exchange rate sampled from a Gaussian distribution $p_0 \sim \mathcal{N}(1, 0.05^2)$. The action space is continuous and one-dimensional, defined as $\mathcal{A} = [-1, 1]$. The interpretation of an action $a_t \in \mathcal{A}$ is twofold: a positive value $a_t \in (0, 1]$ corresponds to the decision to convert a proportion a_t of the current inventory m_t into Currency B; conversely, a non-positive action $a_t \in [-1, 0]$ signifies a “hold” decision where no currency is converted at the current step. The objective is to maximize the cumulative reward, where the reward function is defined as the amount of Currency B obtained at each step. The system dynamics are primarily driven by the stochastic evolution of the exchange rate. To realistically capture mean-reverting market properties, p_t is modeled using an Ornstein-Uhlenbeck (OU) process governed by the following stochastic differential equation:

$$dp_t = \theta(\mu - p_t)dt + \sigma dW_t,$$

where W_t represents a standard Wiener process describing Brownian motion. In the specific implementation, the process parameters are configured as follows: the rate of mean reversion is set to $\theta = 0.05$, the long-term equilibrium price is $\mu = 1.5$, and the volatility coefficient is $\sigma = 0.2$.

Dataset The dataset is generated by a random behavioral policy. This policy adopts a mixture strategy at each time step. Specifically, with a probability of 0.8, the policy executes a non-conversion action (effectively sampling a negative action), opting to hold the current inventory. Conversely, with a probability of 0.2, it selects a conversion action. In this latter case, the specific proportion of currency to be converted is determined by sampling uniformly from the feasible positive action space, thereby introducing stochasticity.

E.1.3 Reference Performance

The normalized score benchmarks an algorithm’s performance on a standardized scale. On this scale, a random policy is set to 0 and an expert policy is set to 100. A score greater than 100 thus signifies that the policy learned from the offline dataset outperforms the online-trained expert policy. The score is computed as follows:

$$\text{score}_{\text{algo}} = 100 \times \frac{\text{performance}_{\text{algo}} - \text{performance}_{\text{expert}}}{\text{performance}_{\text{expert}} - \text{performance}_{\text{random}}}. \tag{15}$$

The reference performance is reported in Table 4.

Table 4: Reference performance across different environments.

Environment	Random Policy	Expert Policy
Halfcheetah	-280.18	12135.0
Hopper	-20.27	3234.3
Walker2d	1.63	4592.3
Offline optimal liquidation	0.0	135.0

E.2 Hyperparameters

Table 5 presents the detailed hyperparameter configurations. For the simpler hopper environment, dynamics models with layer and batch sizes of 256 units are sufficient. However, the increased complexity of walker2d and halfcheetah requires larger architectures with 512-unit layers to ensure convergence.

Table 5: Hyperparameters of PSPO.

Parameter	Value
Dynamics model learning rate	10^{-4}
Policy learning rate	$3 \cdot 10^{-5}$
Critic (Q-value) learning rate	$3 \cdot 10^{-4}$
discounted factor (γ)	0.99
Size of the model ensemble (N)	10
Likelihood Coefficient (β)	1.0
Layer size of policy	256
Layer size of dynamics model	512
Batch size for dynamics model learning	512
Batch size for policy learning	256
Dynamics model training epochs	1000

E.3 Dynamics Model

Following standard model-based RL protocols, we parameterize the transition dynamics using neural networks. Each network takes a state-action pair as input and outputs a Gaussian distribution over the next state and reward, characterized by a predicted mean and diagonal covariance. To effectively capture epistemic uncertainty, we construct a large candidate pool of 100 models, each trained independently via Maximum Likelihood Estimation (MLE) on the offline dataset. During inference, we randomly sample an active ensemble of N models from this pre-trained pool for trajectory prediction.

E.4 Belief Distribution

We construct a dynamics model ensemble and maintain a belief distribution over it. While the prior distribution $P(T)$ over model ensemble can be initialized in various ways to encode specific environmental prior knowledge, practical deployment environments often lack exhaustive initial specifications. It is common practice to initialize the prior as a uniform distribution, which inherently assigns low confidence to OOD regions [5].

E.5 Compute Infrastructure

All computational experiments and benchmarks reported in this study were executed on a high-performance computing workstation designed for large-scale deep learning tasks. The hardware configuration includes:

- GPU Acceleration: A cluster of $8 \times$ NVIDIA GeForce RTX 3090 Ti GPUs, utilized for parallelized ensemble training and policy optimization.
- Processing Unit: An Intel(R) Xeon(R) Platinum 8383C CPU @ 2.70GHz, ensuring efficient data preprocessing and environment simulation.
- Memory: 256 GB of system RAM to accommodate large-scale offline datasets (e.g., D4RL)..

The software environment consists of Ubuntu 20.04 LTS.

F Discussion

From the perspective of policy optimization, PSPO shares structural parallels with Trust Region Policy Optimization (TRPO) [36]. Given the intractability of directly optimizing the original objective, both algorithms resort to constructing a surrogate objective and maximizing it within a localized trust region to ensure stable policy updates. Nevertheless, a key divergence emerges regarding the transition dynamics. Traditional TRPO implicitly

Table 6: Computational overhead.

Method	Train (ms/iteration)	Inference (ms/iteration)
PSPO (Model-based)	112.078±0.619	3.038±0.042
PMDB (Model-based)	80.853±0.408	2.921±0.031
ADM (Model-based)	26.365±0.532	9.162±0.215
DMG (Model-free)	10.618±0.173	1.080±0.030
TD3+BC (Model-free)	7.265±0.140	1.124±0.003

assumes a constant dynamics model T (often represented by sample trajectories). In contrast, PSPO elevates the dynamics to a random variable. By optimizing over a distribution of models $P(T|E)$ rather than a single point estimate, PSPO naturally accounts for epistemic uncertainty, providing a more robust theoretical foundation for policy improvement in non-stationary or data-constrained offline settings.

From the perspective of uncertainty quantification, the proposed framework occupies a unique position at the intersection of Bayesian RL and Risk-averse RL [33, 34, 40, 16]. While Bayesian RL typically addresses epistemic uncertainty by treating transition dynamics as a random variable inferred through posterior beliefs, Risk-averse RL focuses on aleatoric uncertainty to mitigate return stochasticity via risk measures such as CVaR. Unlike standard Bayesian RL which optimizes for expected performance across the belief space, PSPO establishes a foundation for risk-sensitive decision-making. Specifically, the information-theoretic regularization in the E-step serves as a robust prior to mitigate model overfitting, while the guaranteed monotonic improvement in the M-step ensures optimization stability. This mechanism enables the agent to reduce model-induced bias while implicitly safeguarding against distribution shifts. Consequently, PSPO establishes a rigorous foundation for risk-averse policy optimization in safety-critical offline domains. These theoretical properties are empirically validated in Figure 3, which confirms the risk-averse nature of the learned policy.

G Limitation

One limitation of PSPO lies in the computational overhead during training, as generating rollouts requires forward inference across the entire model ensemble. We evaluate the computational costs of recent model-based and model-free methods on identical hardware, with results summarized in Table 6. In general, model-based approaches demand significantly higher training resources than model-free counterparts because of the repetitive ensemble forward passes. PSPO introduces additional overhead beyond standard model-based methods as it requires computing posterior distributions following these forward passes. However, this increased cost is restricted to the training phase. During inference, PSPO remains efficient and comparable to other methods because only the policy network is involved.

H Broader Impact

This work contributes to the field of offline reinforcement learning by providing a framework that improves generalization and robustness in data-driven decision-making. The potential broader impacts include enhancing the efficiency and safety of autonomous systems in domains such as robotics, industrial control, and resource management, where online exploration is often costly. By enabling more reliable policy optimization from static datasets, this research may lead to more sustainable and accessible deployment of AI-driven solutions. There are no specific issues requiring further disclosure.